5350 *Biochemistry* **2010,** *49,* 5350–5357
DOI: 10.1021/bi100317m

BIOCHEMISTRY
including biophysical chemistry & molecular biology
Article

Structural Basis for Promoting and Preventing Decarboxylation in Glutaryl-Coenzyme A Dehydrogenases[†]

Simon Wischgoll,[‡] Ulrike Demmer,[§] Eberhard Warkentin,[§] Robert Günther,[‡] Matthias Boll,*[,‡] and Ulrich Ermler*[,§]

[‡]*Institute of Biochemistry, University of Leipzig, Leipzig, Germany, and* [§]*Max-Planck Institute for Biophysics, D-60438 Frankfurt, Germany*

Received March 3, 2010; Revised Manuscript Received May 20, 2010

ABSTRACT: Glutaryl-coenzyme A dehydrogenases (GDHs) involved in amino acid degradation were thought to catalyze both the dehydrogenation and decarboxylation of glutaryl-coenzyme A to crotonyl-coenzyme A and CO_2. Recently, a structurally related but nondecarboxylating, glutaconyl-coenzyme A-forming GDH was characterized in the obligately anaerobic bacteria *Desulfococcus multivorans* (GDH_{Des}) which conserves the free energy of decarboxylation by a Na^+-pumping glutaconyl-coenzyme A decarboxylase. To understand the distinct catalytic behavior of the two GDH types on an atomic basis, we determined the crystal structure of GDH_{Des} with and without glutaconyl-coenzyme A bound at 2.05 and 2.1 Å resolution, respectively. The decarboxylating and nondecarboxylating capabilities are provided by complex structural changes around the glutaconyl carboxylate group, the key factor being a Tyr → Val exchange strictly conserved between the two GDH types. As a result, the interaction between the glutaconyl carboxylate and the guanidinium group of a conserved arginine is stronger in GDH_{Des} (short and planar bidentate hydrogen bond) than in the decarboxylating human GDH (longer and monodentate hydrogen bond), which is corroborated by molecular dynamics studies. The identified structural changes prevent decarboxylation (i) by strengthening the C4−C5 bond of glutaconyl-coenzyme A, (ii) by reducing the leaving group potential of CO_2, and (iii) by increasing the distance between the C4 atom (negatively charged in the dienolate transition state) and the adjacent glutamic acid.

Glutaryl-coenzyme A (CoA)[1] dehydrogenases (GDHs) belong to the family of FAD-containing acyl-CoA dehydrogenases and are unique in catalyzing both the dehydrogenation and decarboxylation of the acyl-CoA substrate (*1*, *2*). They are involved in the catabolism of lysine, hydroxylysine, and tryptophan in mitochondria and bacteria. Defects in human GDHs cause the inherited neurometabolic disease glutaric acidemia type I (*3*, *4*). GDHs play a different role in anaerobic bacteria that use aromatic growth substrates. Here, many aromatic compounds are channeled to the central intermediate benzoyl-CoA (*5*−*7*). After dearomatization of the latter, ring cleavage, and a series of β-oxidation reactions, glutaryl-CoA is formed which in facultative anaerobes or the Fe(III)-respiring *Geobacter metallireducens* serves as a substrate for decarboxylating GDHs yielding crotonyl-CoA and CO_2 (*8*−*11*).

Decarboxylating GDHs were the subject of various structural and functional studies in the past decade, with the human enzyme (GDH_{hum}) representing the best-studied GDH (*2*, *12*−*17*). Accordingly, the reaction can be separated into the reductive half-reaction, the dehydrogenation of glutaryl-CoA to glutaconyl-CoA (2,3-dehydroglutaryl-CoA), and the decarboxylation half-reaction forming crotonyl-CoA and CO_2 (Figure 1). Similar to those of other acyl-CoA dehydrogenases, the reaction is initiated by the abstraction of the *pro-R* proton from the C2 atom by a glutamate carboxylate which acts as general catalytic base and is conserved in all GDHs (Glu370 in GDH_{hum}). In the next step, a hydride is transferred from the C3 atom to the N5 atom of the FAD cofactor. Decarboxylation of glutaconyl-CoA proceeds via a dienolate transition state, which in GDH_{hum} is protonated directly or solvent-mediated by Glu370, thereby regenerating the glutamate base (*18*) (Figure 1). The release of crotonyl-CoA is the rate-limiting step of GDH_{hum} (*16*). The structures of GDH_{hum} in the

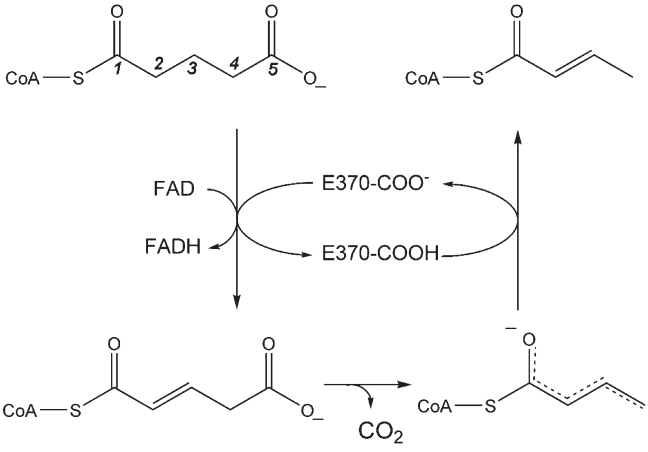

FIGURE 1: Reaction catalyzed by glutaryl-CoA dehydrogenases: dehydrogenation reaction and decarboxylation reaction. A conserved glutamate residue serves as a proton acceptor during the dehydrogenation reaction and as a direct or indirect proton donor for the protonation of the dienolate transition state.

[†]This work was supported by German Research Council (DFG) Project BO 1565/8-1 and the Max-Planck Gesellschaft.

*To whom correspondence should be addressed. U.E.: phone, +49-69-63031054; fax, +49-69-63031002; e-mail, ulrich.ermler@biophys.mpg.de. M.B.: phone, +49-341-9736996; fax, +49-341-9736910; e-mail, boll@uni-leipzig.de.

[1]Abbreviations: CoA, coenzyme A; GDH, glutaryl-CoA dehydrogenase; GDH_{hum}, GDH from *Homo sapiens*; GDH_{Des}, GDH from *Desulfococcus multivorans*; rmsd, root-mean-square deviation.

 Published on Web 05/20/2010

Table 1: Crystallization, Data Collection, and Refinement of GDH_{Des} Structures

	GDH	GDH−glutaryl-CoA	GDH−CoA
	Crystallization		
reservoir solution	50% (v/v) MPD, 0.1 M Tris (pH 8.5), 0.2 M $NH_4H_2PO_4$	15% (v/v) MPD, 0.1 M imidazole (pH 6.5), 0.2 M KCl, 2% PEG 3350	8% (v/v) ethylene glycol, 0.1 M MES (pH 6.5)
	Data Collection		
wavelength (Å)	1.0000	0.9999	0.9918
space group	$P2_12_12$	$C2$	$I4_1$
unit cell parameters			
a, b, c (Å)	62.6, 152.3, 251.0	175.0, 114.8, 122.2	123.7, 123.7, 112.3
α, β, γ (deg)		134.0	
no. of tetramers per asymmetric unit	1.5	2 × 0.5	0.5
resolution range (Å)	50−2.1 (2.16−2.1)[a]	50.0−2.05 (2.15−2.05)[a]	50.0−2.7 (2.8−2.7)[a]
redundancy	6.0 (5.2)[a]	3.1 (3.1)[a]	5.2 (5.4)[a]
completeness (%)	99.7 (98.0)[a]	96.5 (96.6)[a]	95.3 (97.1)[a]
R_{merge} (%)	11.3 (56.7)[a]	5.8 (51.9)[a]	8.9 (84.8)[a]
$I/\sigma(I)$	11.0 (3.1)[a]	12.3 (3.2)[a]	10.5 (2.4)[a]
	Refinement		
resolution limit (Å)	30−2.1 (2.154−2.1)[a]	30−2.05 (2.1−2.05)[a]	30−2.7 (2.77−2.70)[a]
R_{work}/R_{free} (%)	17.9/22.1 (24.9/29.0)[a]	18.4/22.3 (32.8/35.4)[a]	18.7/25.2 (30.3, 44.0)[a]
no. of residues, FAD, CoA compound	6 × 389, 6, 0	4 × 389, 4, 4 (glutaconyl-CoA)	2 × 389, 2, 1.5 (CoA)
no. of solvent molecules	791, 6 Cl^-	478	14
rmsd for bond lengths (Å)	0.017	0.013	0.009
rmsd for bond angles (deg)	1.67	1.54	1.26
average B (Å^2) (protein/FAD/CoA/solvent)	38/28/−/36	53/44/54/56	84/69/87/73

[a]Data in parentheses are for the highest-resolution shell.

presence of the dehydrogenated product or transition state analogues 4-nitrobut-2-enoyl-CoA (*14*) or 3-thiaglutaryl-CoA (*17*) provided detailed insights into the mechanism of the dehydrogenation and decarboxylation partial reactions. A network of conserved amino acid functionalities was proposed to polarize the C4−C5 bond to initiate decarboxylation. The invariant Arg94, hydrogen bonded to the carboxylate of the reduced substrate, was shown to play a key role in the decarboxylation process (*13*, *14*).

Very recently, a nondecarboxylating GDH from the sulfate-reducing, aromatic compound-degrading bacteria *Desulfococcus multivorans* (GDH_{Des}) was purified and characterized (*11*). Because of the poor energy yield of this organism (*19*), the exergonic decarboxylation of the glutaconyl-CoA intermediate released by GDH is accomplished by a membrane-bound, Na^+-pumping glutaconyl-CoA decarboxylase (*20*−*22*). Amino acid sequence comparisons revealed that GDH_{Des} contains the glutamate general base catalyst (Glu367, GDH_{Des} numbering) and the invariant arginine (Arg87) involved in carboxylate binding. However, the active site amino acids Glu87, Ser95, and Tyr369 (GDH_{hum} numbering), present in all decarboxylating GDHs, were exchanged in GDH_{Des}. For this reason, the presence or absence of these amino acids was hypothesized to govern whether the glutaconyl-CoA intermediate is further decarboxylated or released (*11*).

In the work presented here, the crystal structure of the non-decarboxylating GDH_{Des} was determined with and without the oxidized product of the natural substrate at 2.05 and 2.1 Å resolution, respectively. While the structural basis for the dehydrogenation partial reaction appears to be similar in all GDHs and other acyl-CoA dehydrogenases, a number of unique features at the active site of GDH_{Des} were identified that are proposed to ensure the prevention of decarboxylation. Prevention of decarboxylation by GDHs appears to be essential for aromatic compound-degrading obligate anaerobes with a poor energy yield as they rely on energy conversion by Na^+-pumping glutaconyl-CoA decarboxylases.

MATERIALS AND METHODS

Heterologous Expression and Purification of His-Tagged GDH_{Des}. The gene encoding GDH_{Des} (gi 228015642) was expressed in *Escherichia coli* according to the procedure described recently (*11*). The expressed His-tagged gene product was purified as described from the supernatant at 4 °C by Ni-Sepharose high-performance chromatography. The purity of the enzyme was >98% as estimated by sodium dodecyl sulfate−polyacrylamide gel electrophoresis. The amount of flavin and protein in glutaryl-CoA dehydrogenase was determined as described previously (*11*).

Crystallization and Data Collection for GDH_{Des}. Prior to crystallization, GDH was concentrated to approximately 35 mg/mL in 10 mM 2-(*N*-morpholino)ethanesulfonic acid (MES) (pH 6.5), 0.5 M KCl, 10% (w/v) glycerol, 1 mM dithiothreitol, and 1 mM FAD. Crystallization trials were performed with the hanging drop vapor diffusion method at a temperature of 4 °C using a sparse matrix crystallization kit (Jena Bioscience GmbH) for initial screening. The best crystals for native GDH were obtained after equal volumes of the enzyme solution (10 mg/mL) had been mixed with the reservoir solution containing 50% (v/v) MPD, 0.1 M Tris-HCl (pH 8.5), and 0.2 M $NH_4H_2PO_4$. The GDH_{Des} substrate−product complex was crystallized using the enzyme solution (20 mg/mL) supplemented with 2 mM glutaryl-CoA (previously adjusted to pH 6.0) and a reservoir solution of 15% (v/v) MPD, 0.1 M imidazole (pH 6.5), 0.2 M KCl, and 2% PEG 3350. Crystals emerged after 2 days and were immediately frozen using the reservoir buffer supplemented with

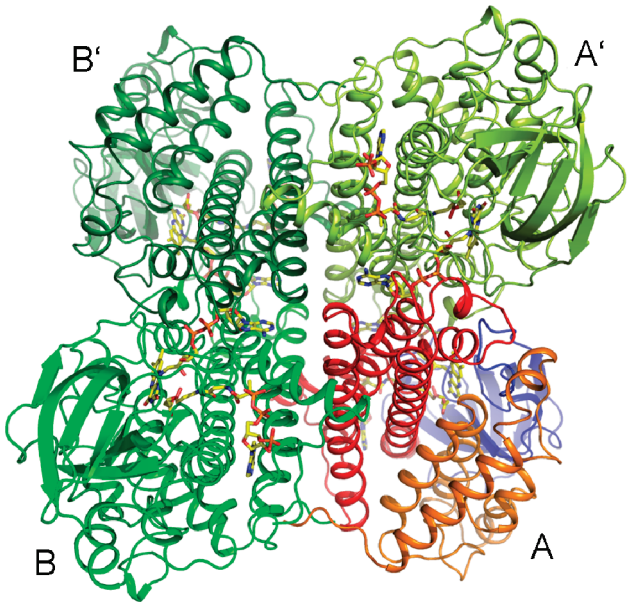

FIGURE 2: Structure of the binary GDH−glutaconyl-CoA complex of *D. multivorans*. The tetrameric enzyme is composed of a dimer of dimers (A−B and A′−B′). Each subunit consists of an α-helical domain (orange), a *β*-sheet domain (blue), and another α-helical domain (red). FAD and glutaconyl-CoA (drawn as stick models) are embedded between the three domains of one subunit and one domain of the partner subunit.

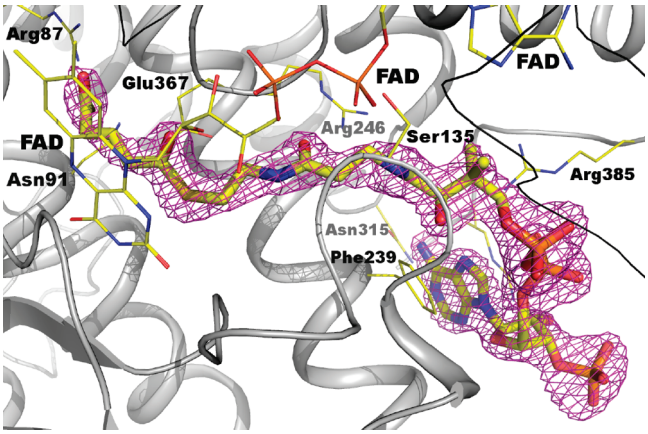

FIGURE 3: Glutaconyl-CoA binding site. Glutaconyl-CoA is shown together with its $2F_{obs} - F_{calc}$ electron density (contour level of 1.5σ) to demonstrate its high quality, which allows the presented mechanistic interpretations. In addition, FAD and the most important residues that interact with glutaconyl-CoA are drawn as a stick model.

20% 1,2-propanediol (by volume). Data for GDH_{Des} and the GDH_{Des}−glutaconyl-CoA complex were collected at the SLS-PXII beamline in Villigen, Switzerland, to resolutions of 2.05 and 2.1 Å, respectively. Processing and scaling were performed using HKL (*23*) and XDS (*24*), respectively (see Table 1).

Phase Determination and Refinement. The structures were determined by the molecular replacement method using PHASER (*25*), and the coordinates of GDH_{hum} [Protein Data Bank (PDB) entry 1siq] (*14*) as the first search model. Iterative cycles of refinement and manual model building were performed with REFMAC5 (*26*) and COOT (*27*). TLS refinement, treating each monomer as a separate TLS group, maximum likelihood minimization with isotropic *B* value refinement, and several modifications of the geometry files of the substrate led to the final result listed in Table 1. Structure interpretation was based on normalized $2F_{obs} - F_{calc}$ and $F_{obs} - F_{calc}$ electron density maps. The quality of the model was checked with PROCHECK (*28*). Figures 2−5 were produced with PYMOL (Schrödinger, LLC). The coordinates of GDH_{Des} and the GDH_{Des}−glutaconyl-CoA complex were deposited in the Protein Data Bank as entries 3MPI and 3MPJ, respectively.

Preparation of Site-Directed Mutants. Point mutations were inserted into the gene of GDH_{Des} and cloned in the expression plasmid in a single step (*29*). Point mutations were introduced by polymerase chain reaction (PCR) using the QuikChange site-directed mutagenesis kit (revision B, Stratagene) using appropriate mutagenesis primers (Table S1 of the Supporting Information). The wild-type plasmid, which served as a template, was digested with *Dpn*I (FastDigest DpnI, Fermentas). The digested PCR mixture was separated by gel electrophoresis on a 1% agarose gel. The plasmid was extracted (GenElute Gel Extraction Kit, Sigma-Aldrich) and transformed into chemically competent *E. coli* TOP10 cells (Invitrogen). Transformed cells were cultured overnight at 37 °C in Luria-Bertani agar with the appropriate antibiotic. Single colonies were selected and cultured in Luria-Bertani medium for plasmid propagation. The plasmid was isolated (GenElute Plasmid Miniprep Kit, Sigma-Aldrich), and the mutated insert with flanking regions was sequenced after sequencing PCR by the chain termination method with appropriate primers (Table S1) on an ABI Prism 3730 Genetic Analyzer (Amersham Pharmacia Biotech). For the insertion of further point mutations, plasmids with one mutation were used as the template. Expression of the mutated genes and purification of the His-tagged proteins were conducted as described previously (*11*).

Enzyme Assays and Kinetic Studies. Enzyme activity was determined at 30 °C in a continuous spectrophotometric assay containing 50 mM Tris-HCl (pH 7.8), 250 mM KCl, and 0.2 mM ferrocenium hexafluorophosphate. The reaction was started via addition of glutaryl-CoA (200 μM), and the time-dependent reduction of ferrocenium hexafluorophosphate was monitored at 300 nm ($\Delta\varepsilon_{300}$ = 3600 M^{-1} cm^{-1}) (*11*). For the determination of K_m values, the glutaryl-CoA concentration was varied from 1 to 500 μM (two to three determinations with each concentration); the values obtained were fitted to Michaelis−Menten curves using Prism Graphpad (Graphpad Software Inc., La Jolla, CA). For the qualitative determination of substrate consumption and product formation, samples were taken in a discontinuous assay at different time points and analyzed by reversed-phase HPLC analysis as described previously (*11*). Glutaryl-CoA, glutacanoyl-CoA, and crotonyl-CoA served as standards.

Sequence Analysis and Molecular Modeling. Sequence analysis studies were initiated by a Blast search (*30*) with the sequence gi 228015642 as the query. The default parameters were applied. The 500 resulting sequences were filtered for the occurrence of the conserved Arg87, which has been shown to be characteristic for GDH enzymes (*13*). The 43 resulting sequences were aligned with ClustalW (*31*), and an average distance tree based on the Blosum62 matrix was calculated with JalView version 2.4.0 (*32*).

Molecular dynamics studies were used for the GDH_{Des}− and GDH_{hum}−glutaconyl-CoA complex structures using the Molecular Operating Environment MOE (2008.10, Chemical Computing Group, Inc., Montreal, QC). For the latter, the substrate 3-thiaglutaryl-CoA (*17*) was modified to glutaconyl-CoA. Prior to calculation, the water molecules were stripped off and hydrogen atoms were added. Moreover, Amber99 charges were assigned to

each atom and the positions of the hydrogen atoms were relaxed by a steepest descent minimization of 100 steps keeping the heavy atoms of the structure fixed. The Amber99 force field was used with a distance-dependent dielectric constant. The simulations were performed for 1 ns at 300 K with a time step of 2 fs with the default parameters. Snapshots were saved every 1 ps.

RESULTS AND DISCUSSION

Overall Structure. The structures of GDH_{Des} with and without glutaconyl-CoA were determined by the molecular replacement method with human GDH (PDB entry 1siq) as the model and subsequently refined to R_{free} values of 22.1 and 22.3% at resolutions of 2.05 and 2.1 Å, respectively (Figure 2 and Table 1). As GDH_{Des} showed a tendency to lose the flavin cofactor, the protein solution was supplemented with 1 mM FAD during the entire crystallization process. Under these conditions, the FAD binding site was completely occupied in all subunits of the asymmetric unit in both structures. The CoA ester compound was present at a high occupancy in all four subunits of the asymmetric unit of the binary complex. The electron density of the acyl moiety of the CoA ester was only insignificantly weaker than that of the residual molecule, indicating that partial hydrolysis during the crystallization process was greatly prevented (Figure 3). Suppression of hydrolysis was the major challenge of cocrystallization as the electron density calculated from most data sets of GDH_{Des} cocrystallized in the presence of 5 mM glutaryl-CoA solely contained CoA (Table 1, GDH−CoA). The rather planar shape of the electron density of the acyl-CoA group (Figure 3) prompted us to model the CoA ester as glutaconyl-CoA, the product of the redox half-reaction. This assumption is in agreement with the structure of the CoA ester compound in the isobutyryl-CoA dehydrogenase binary complex (*33*). Obviously, the redox reaction proceeded in the crystallization solution, which has also been described for GDH_{hum} (*14*). We assume that the thereby generated $FADH_2$ was reoxidized with molecular O_2 during crystallization.

GDH_{Des} is present in a homotetrameric oligomeric state consisting of a dimer of two tightly associated dimers. Each subunit is composed of an amino-terminal α-helical bundle domain of six α-helices, a medial seven-strand *β*-sheet domain (strands 1−7), and a second α-helical domain of five α-helices at the carboxy terminus (Figure 2). This architecture corresponds to that described for GDH_{hum} and other acyl-CoA dehydrogenases with a rmsd between GDH_{Des} and GDH_{hum} of 1.6 Å (95% of the C_α atoms). The relatively low level of sequence identity of 27% between GDH_{Des} and GDH_{hum} is reflected by diverse structural differences especially in loop segments. However, only the three described in the following appear to be functionally relevant.

First, the orientation of the irregular segment at the N-terminal end proceeding α-helix 6:27 differs by more than 90° between GDH_{Des} and GDH_{hum}. Whereas in GDH_{hum} the elongated N-terminal arm (15 residues) interacts with several parts of the C-terminal domain of a subunit of the counter dimer, the four N-terminal residues of GDH_{Des} are multiply linked with the same residues of the partner subunit. Correct oligomerization is essential for the functionality of GDHs or other acyl-CoA dehydrogenases documented by several pathogenic mutations in interface regions (*33*). Second, the six or seven terminal residues of the C-terminal arms of GDH_{Des} and GDH_{hum} are also oriented perpendicular to each other. In GDH_{Des}, this irregular segment pivots toward the loop between α-helices 233:271 and 284:310 of the same subunit, thereby shielding the adenosine moiety of CoA from bulk solvent. In contrast, the C-terminal arm of GDH_{hum} is attached to the partner subunit and encapsulates the adenine base of FAD. Third, parts of α-helix 233:271 and concomitantly α-helix 284:310 (attached to helix 233:271) of GDH_{Des} are displaced ~1.5 Å toward the active site cleft. As a result, the binding site of the glutaconyl group of the CoA compound becomes narrower.

FAD Binding and Substrate and Product Binding. FAD and glutaconyl-CoA are embedded in an approximately 15 Å deep cleft formed by the three domains of one subunit and the C-terminal domain of the partner subunit as described for other acyl-CoA dehydrogenases (Figure 3). FAD binds to GDH_{Des} in an extended conformation with a planar isoalloxazine ring. Its overall conformation and polypeptide−FMN interactions are well-conserved between GDH_{Des} and GDH_{hum} and among members of the acyl-CoA dehydrogenase family. Significant differences are found with respect to adenosine binding. For example, the ribose hydroxyl groups of GDH_{hum} are linked to the polypeptide via Asp343 and Asp374, whereas in GDH_{Des}, only Asn371 is available as a binding partner. As mentioned, the adenine ring of FAD in GDH_{Des} is highly accessible to bulk solvent, whereas in GDH_{hum}, the adenine is hydrogen-bonded to the C-terminal arm and thereby encapsulated. Although partly compensated by Phe281 (Asn285 in GDH_{hum}), which is attached parallel to the adenine ring, the lack of interaction with the C-terminal arm might be responsible for the rather weak FAD binding in GDH_{Des}.

Glutaconyl-CoA binds to the protein in the well-conserved J-shaped conformation and is similarly positioned as the CoA compounds in other acyl-CoA dehydrogenases (Figure 3). However, a comparison between glutaconyl-CoA binding in GDH_{Des} and 4-nitrobut-2-enoyl-CoA or 3-thiaglutaryl-CoA binding in GDH_{hum} (*14*, *17*) revealed substantial conformational changes throughout the molecule. Most notable is the sharper bend of the J-shaped CoA in GDH_{hum} compared to GDH_{Des} that implies a displacement of the 3′-phosphoryl group of the adenosine by more than 3 Å in the superimposed binary complexes. In GDH_{Des}, the loop between α-helices 233:271 and 284:310 (implying a small shift of α-helix 284:310) is displaced up to 6 Å to contact the less bent 3′-phosphorylated adenosine and to allow an attachment of the C-terminal arm to this loop. In this conformation, the adenine ring is sandwiched between Arg389 of the C-terminal arm and Phe239 of α-helix 233:271 (Figure 3). Glutaconyl-CoA binding does not induce large-scale conformational changes in the polypeptide. Only side chains were adjusted up to a size of 1 Å except for those of Arg385 and Arg389 that rotate toward glutaconyl-CoA. The empty space in the cavity of the substrate-free structure is filled with several firmly bound solvent molecules.

The modes of binding of the glutaconyl and 4-nitrobut-2-enoyl groups of GDH_{Des} and GDH_{hum} were analyzed in detail (Figures 4 and 5). The thioester oxygen in GDH_{Des} forms two hydrogen bonds to the 2′-OH group of FAD and the peptide amide group of Glu367, and both are strictly conserved within the acyl-CoA dehydrogenase family (*34*). Likewise, the C2 atom of glutaconyl-CoA is always in close contact with the carboxylate group of the invariant glutamate. The distance between the C2 and Glu367 $O_{\varepsilon 2}$ atoms is 3.2 Å in GDH_{Des} and 3.3 Å in GDH_{hum}. Notably, the $O_{\varepsilon 2}$ atom also appears to contact the C4 atom in GDH_{hum} (3.3 Å) but not in GDH_{Des} (3.7 Å). In GDH_{Des}, however, the carboxylate group of Glu367 is additionally hydrogen-bonded to the hydroxyl

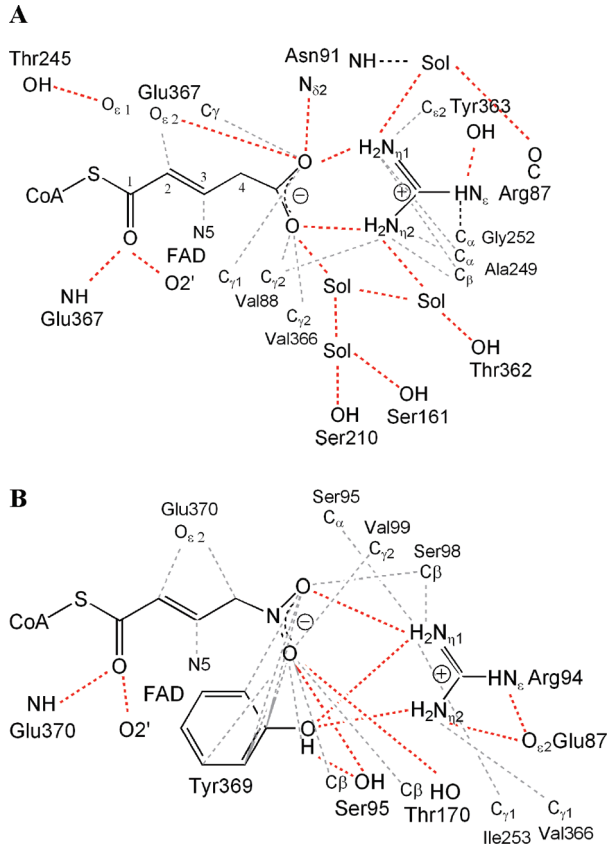

FIGURE 4: Schematic representation of the interactions between the carboxylate group of glutaconyl-CoA and GDH_{Des} (A) and the nitro group of 4-nitrobut-2-enoyl-CoA and GDH_{hum} (B). Polar (nonpolar) interactions are drawn as red (gray) dashed lines. Solvent is abbreviated Sol. Polar interactions between the carboxylate of glutaconyl-CoA and the polypeptide dominate in nondecarboxylating GDH and nonpolar interactions in decarboxylating GDHs.

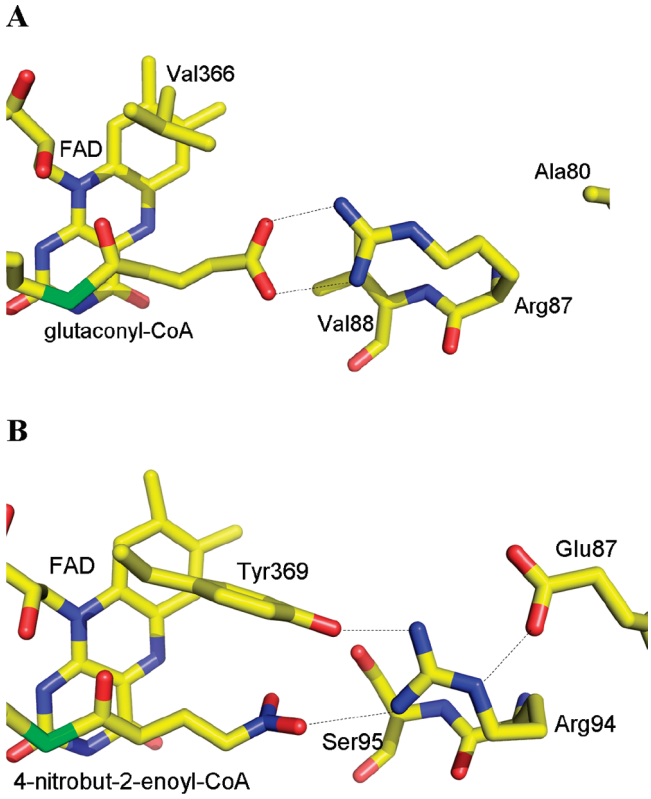

FIGURE 5: Conformations of residues that crucially influence decarboxylation and nondecarboxylation in GDH_{Des} (A) and GDH_{hum} (B). The different interaction between the carboxylate group of glutaconyl-CoA and the guanidinium group of Arg87 or Arg94 mainly triggered by V366Y exchange is the major structural feature for the different catalytic behavior of GDH_{Des} and GDH_{hum}. Val366, Val88, and Ala80 of GDH_{Des} were exchanged for tyrosine, serine, and glutamate, respectively, in site-specific mutagenesis experiments.

group of Thr245. In all structurally characterized acyl-CoA dehydrogenases, the C3 atom is in van der Waals contact with the N5 atom of FAD, their separation being 3.2 Å in GDH_{Des}. Surprisingly, in the GDH_{hum}−4-nitrobut-2-enoyl-CoA complex, this distance is with 3.9 Å too long for an efficient hydride transfer reaction (*14*), in contrast to the corresponding distance in the GDH_{hum}−3-thiaglutaryl-CoA complex of 3.5 Å (*17*). Because of this ambiguity, we compared the structures between both GDH_{hum}−substrate analogue complexes and the GDH_{Des}−glutaconyl-CoA complex, although the analogy between the isosteric and isoelectronic glutaconyl and 4-nitrobut-2-enoyl groups is stronger than that between the glutaconyl and 3-thiaglutaryl groups.

The carboxylate and nitro groups of the glutaconyl and 4-nitrobut-2-enoyl moieties, respectively, are anchored multiply to the protein matrix (Figures 4 and 5). The most pronounced interaction in GDH_{Des} is a bidentate hydrogen bond between both carboxylate oxygens and the $N_{\eta 1}$ and $N_{\eta 2}$ atoms of Arg87, with the conjugated carboxylate and guanidinium groups being nearly planar. The short distance between the interacting atoms and the relatively nonpolar surrounding of the guanidinium group maintaining a high local charge density argue for a strong ionic interaction. In contrast, the equivalent Arg94 in GDH_{hum} forms a monodentate hydrogen bond to the nitro and carboxylate oxygens of the 4-nitrobut-2-enoyl and 3-thiaglutaryl groups, respectively (*14*, *17*). This finding is a consequence of the rather orthogonal arrangement of the nitro/carboxylate and guanidinium planes in GDH_{hum} (Figures 4 and 5). Furthermore, the positive charge on the guanidinium group in GDH_{hum} is more delocalized as in GDH_{Des}, in particular, by a salt bridge to Glu87 (Ala80 in GDH_{Des}) and a bifurcated hydrogen bond to the side chain oxygen of Tyr369 (Val366 in GDH_{Des}) (Figures 4 and 5). Tyr369, additionally, compresses the Arg94 side chain to a less elongated conformation, which increases the distance between the guanidinium nitrogens and the nitro/carboxylate oxygens and thereby decreases the strength of the binding between them.

The conformation of the glutaconyl-CoA carboxylate and its interactions with Arg87 (Arg94 in GDH_{hum}) were further analyzed by molecular dynamics studies using the Molecular Operating Environment, MOE. Throughout the full simulation time of 1 ns, the position of glutaconyl-CoA in GDH_{Des} remained unaffected, which is documented by a rmsd of < 1 Å relative to the X-ray structure (data not shown). In comparison, GDH_{Des} equipped with glutaconyl-CoA in the conformation of GDH_{hum} readily returns to the conformation of the crystal structure. The inverted result was obtained with GDH_{hum} via application of glutaconyl-CoA in the conformation found in GDH_{Des} and thus corroborates the X-ray crystallographic findings that the specific protein environments around the carboxylate in GDH_{Des} and GDH_{hum} adjust a bidentate and monodentate binding mode, respectively.

Apart from this pronounced difference, the number of polar interactions between the carboxylate/nitro functionalities of the CoA compound and the polypeptide are virtually balanced in GDH_{Des} and GDH_{hum}. In GDH_{Des}, one of the carboxylate

Table 2: Properties of Site-Directed Mutants of GDH_{Des}

	decarboxylation	dehydrogenation	mol of FAD per monomer	K_m (μM)	V_{max} (μmol min^{-1} mg^{-1})	V_{max} (% activity)	k_{cat}/K_m (s^{-1} μM^{-1})	tetramer: monomer ratio[a]
wild type	−	√	0.65	53 ± 4	3.4 ± 0.1	100	1.7	8.2:1
A80E	−	−	< 0.1	−	< 0.001	−	−	8.5:1
V88S	−	√	0.66	59 ± 13	0.27 ± 0.02	8.0	0.12	8.8:1
V366Y	−	√	< 0.1	28 ± 6	0.032 ± 0.001	0.9	0.01	5.3:1
A80E/V366Y	−	√	< 0.1	14 ± 4	0.05 ± 0.003	1.5	0.01	10.1:1
A80E/S161T/V366Y	−	−	< 0.1	−	< 0.001	−	−	12.8:1

[a]The tetramer:monomer ratio was determined by gel filtration, and the amount of dimer formed was negligible.

oxygens is additionally hydrogen-bonded to the $N_{\delta 2}$ atom of Asn91 and the other via solvent molecules to hydroxyl groups of Ser120, Ser161, and Thr362. For comparison, the nitro oxygens are hydrogen-bonded to the hydroxyl group of Ser95 and Thr170 in GDH_{hum} (Figure 4). In contrast, the nonpolar interactions between the polypeptide and the nitro/carboxylate oxygen atoms dominate in GDH_{hum} compared to GDH_{Des}, indicating a more hydrophobic environment.

Because of the different protein environments, the conformation and position of the glutaconyl and 4-nitrobut-2-enoyl (3-thiaglutaryl) groups also differ in GDH_{hum} and GDH_{Des} (Figures 4 and 5). In GDH_{Des}, the conformation of the glutaconyl group is characterized by a bend between the C4 and C5 atoms which turns the carboxylate group away from the *re* side of FAD and thereby optimizes its interaction with Arg87. The plane of the carboxylate group approximately corresponds to the plane of the CoA thioester. This conformation significantly deviates from that of the 4-nitrobut-2-enoyl group of GDH_{hum}, which is rather straight, and the nitro plane is oriented perpendicular to that of the thioester. In the GDH_{hum}−3-thiaglutaryl complex, the carboxylate conformation lies between that of the GDH_{hum}−4-nitrobut-2-enoyl-CoA and GDH_{Des}−glutaconyl-CoA complexes (*14*, *17*). The described conformational differences seem to be mainly due to the Y369V exchange: in GDH_{hum}, the bulky phenol moiety of Tyr369 displaces the 4-nitrobut-2-enoyl (3-thiaglutaryl) group and causes a reorientation of the nitro (carboxylate) oxygens; as a consequence, the distance to Arg94 is increased, that to the proton donor Glu370 is decreased, and the bidentate hydrogen bond to Arg87 in GDH_{Des} is replaced by a monodentate bond in GDH_{hum} (Figure 4). The key function of Tyr369 is further substantiated by sequence comparison studies; 43 glutaryl-CoA dehydrogenase sequences identified on the basis of the strictly conserved Arg87 (missing in other acyl-CoA dehydrogenases) cluster into two major groups (Figure S1 of the Supporting Information). The first group (34 members) contains a tyrosine at position 369 (GDH_{hum} numbering), which is exchanged with a valine in the second group. The nine members of the second group were exclusively found in obligately anaerobic Deltaproteobacteria/Gram-positives that also contain the genes of glutaconyl-CoA decarboxylases not present in the 34 organisms with GDHs of the first group.

Catalytic Reaction. (*i*) *Redox Reaction*. The structure of the GDH_{Des}−glutaconyl-CoA complex is completely compatible with the mechanism of the reductive half-reaction established for acyl-CoA dehydrogenases, which is characterized by the rupture of two kinetically stable C−H bonds. The substrate binds to the *re* side of the FAD ring, and the C2−C3 bond is sandwiched between the carboxylate group of Glu367 and the pyrimidine ring of FAD. Then, the C3 *pro-R* hydride and the C2 *pro-R* proton are abstracted in an antiperiplanar arrangement by the N5 atom of oxidized FAD and by the glutamate carboxylate group, respectively. The C2 atom is acidified ($pK_a \sim 8$) because of its conjugation to the thioester carbonyl group which is polarized via two hydrogen bonds conserved in all acyl-CoA dehydrogenases (*34*).

(*ii*) *Decarboxylation Reaction*. In general, the transition state energy for the decarboxylation of glutaconyl-CoA is reduced by the stabilization of the anionic dienolate intermediate, the positioning of a suitable proton donor in the vicinity of the C4 atom, the formation of a favorable surrounding for the neutral CO_2 leaving molecule, and the weakening of the C4−C5 bond. Comparison of the GDH_{Des} and GDH_{hum} binary complexes offers valuable information to improve our understanding of their distinct decarboxylation behavior.

GDH_{hum} and GDH_{Des} share the ability to neutralize the dienolate state by delocalizing the charge via the stabilized oxyanion of the thioester, as both require it for the redox reaction (Figure 4). In GDH_{hum}, protonation of the dienolate anion generated after decarboxylation was originally attributed directly to the protonated Glu370 facilitated by a 1,3-prototropic shift (*15*, *35*), whereas recent results argue for a more indirect solvent-mediated protonation process (*18*). In each case, efficient proton donation is favored by the shorter distance between the glutaconyl C4 and Glu370 OE2 atoms in GDH_{hum} compared to GDH_{Des} which is mainly a consequence of the displacement of the CoA moiety by the bulky side chain of Tyr369 (Figure 4).

The environment of the glutaconyl carboxylate group is significantly different in GDH_{hum} and GDH_{Des}. In GDH_{Des}, the fraction of polar interactions between the carboxylate group and the protein matrix is greater and the fraction of nonpolar interactions is smaller (see Figure 4) as in GDH_{hum} favoring the binding of the charged carboxylate in GDH_{Des} and a neutral CO_2 in GDH_{hum}. The strong bidentate (GDH_{Des}) and the rather weak monodentate (GDH_{hum}) hydrogen bonds between the carboxylate and the invariant arginine largely determine this difference.

The more planar arrangement of the carboxylate group in GDH_{Des} relative to the double bond and the thioester plane would support the formation of an extended conjugated sp^2 system that strengthens the C4−C5 bond and thus represses the cleavage. Moreover, the strong interaction between the carboxylate group and the guanidinium group of Arg87 in GDH_{Des} (Figure 5) withdraws electron density from atom C5 toward the oxygen atoms and from atom C4 toward atom C5, which impedes the cleavage of the C4−C5 bond.

Site-Directed Mutants of GDH. Amino acid sequence comparisons and the structural information obtained in this work suggested that only a relatively small number of exchanges of amino acids in GDH_{Des} determine decarboxylation activity.

Of potential interest were especially the exchange of V366Y and A80E, with the tyrosine and glutamate both being strictly conserved in decarboxylating GDHs. An exchange of Arg87 was not conducted because of its conservation in both GDH types and its great effect on K_m and k_{cat} in GDH_{hum} (*13*). Accordingly, the A80E, V366Y, and, in addition, V88S and corresponding double/triple mutants were constructed to convert GDH_{Des} to a decarboxylating enzyme. All mutated GDH_{Des} forms were expressed in a soluble form and in a predominantly tetrameric oligomerization state, the latter being analyzed by gel filtration experiments (Table 2). Obviously, the structural integrity of GDH is not influenced by the mentioned amino acid exchanges. Similar to the wild-type enzyme, a minor fraction (< 15%) of the mutated proteins eluted as a monomer probably due to dissociation during dilution. Kinetic properties and the content of the FAD cofactor were determined as summarized in Table 2.

With the exception of V85S, all enzyme variants essentially lost the FAD cofactor; in the case of the V366Y mutant and A80E/V366Y double mutant, a residual activity was determined in the presence of 0.5 mM FAD in the assay buffer. Surprisingly, these two mutants exhibited a slight but significant decrease in the K_m values, indicating an interaction between Tyr366 and glutaryl-CoA, which can be understood on the basis of the structural data. The low FAD content could be structurally rationalized for the V366Y mutant because of weak interference between its phenol ring and FAD. In none of the mutated GDHs was the conversion to a decarboxylating GDH_{Des} accomplished, but their properties indicated the complexity of constructing a bifunctional enzyme with two spatially adjacent active sites.

CONCLUSIONS

The growth of sulfate-reducing or -fermenting bacteria with organic acids and aromatics is thermodynamically limited by a poor energy metabolism. Therefore, these bacteria are obliged to employ enzymes that conserve the energy of exergonic reactions wherever feasible. In the case of glutaryl-CoA decarboxylation, the combined action of a nondecarboxylating GDH and Na^+-pumping glutaconyl-CoA decarboxylase guarantees that the free energy of decarboxylation [−30 kJ/mol under cellular conditions (*22*)] is conserved in the form of an electrochemical gradient. The presented structure of the GDH−product complex provides a solid molecular basis for how glutaconyl-CoA decarboxylation is efficiently prevented in obligate anaerobes with a poor energy yield.

The binding site of the glutaconyl-CoA carboxylate group in GDH_{hum} and GDH_{Des} significantly differs, and specific structural features modify the strength of the C4−C5 bond, the stability of the proposed dienolate transition state, and the leaving group potential of CO_2. The key player of the thereby generated different catalytic behavior appears to be a strictly conserved tyrosine in decarboxylating GDHs (Tyr369 in GDH_{hum}), which is replaced with a valine in nondecarboxylating GDHs (Val366 in GDH_{Des}) (Figures 4 and 5 and Table 2). The bulky side chain of Tyr369 at the active site in GDH_{hum} (i) prevents a shorter distance between Arg94 and the carboxylate moiety of glutaconyl-CoA, (ii) displaces the glutaconyl group toward Glu370, (iii) adjusts the orientation of the carboxylate oxygens, and (iv) reduces the polarity of the substrate carboxylate site. In particular, the weaker interaction between the glutaconyl carboxylate group and Arg94, which is strongly enhanced by Glu87, is responsible for the decarboxylating activity of GDH_{hum} (Figures 4 and 5).

Mutagenesis experiments with the aim of constructing a GDH_{Des} with a decarboxylation activity revealed the complexity of this venture. The V366Y and A80E mutations of key residues in GDH_{Des} altered both FAD binding and concomitantly stability, as well as substrate binding, which can be partly rationalized on the basis of the presented structure. For this reason, a rational choice of promising amino acid exchanges is difficult because unpredictable conformational changes easily disturb the complex network of interactions required for substrate and flavin binding, and for the dehydrogenation reaction.

ACKNOWLEDGMENT

We thank Hartmut Michel for continuous support and the staff of PXII at the Swiss-Light-Source in Villigen, Switzerland, for help during data collection.

SUPPORTING INFORMATION AVAILABLE

Primers used for PCRs in the mutagenesis experiments (Table S1) and average distance tree of decarboxylating and nondecarboxylating GDHs (Figure S1). This material is available free of charge via the Internet at http://pubs.acs.org.

REFERENCES

1. Lenich, A. C., and Goodman, S. I. (1986) The purification and characterization of glutaryl-coenzyme A dehydrogenase from porcine and human liver. *J. Biol. Chem. 261*, 4090–4096.
2. Westover, J. B., Goodman, S. I., and Frerman, F. E. (2001) Binding, hydration, and decarboxylation of the reaction intermediate glutaconyl-coenzyme A by human glutaryl-CoA dehydrogenase. *Biochemistry 40*, 14106–14114.
3. Goodman, S. I., Stein, D. E., Schlesinger, S., Christensen, E., Schwartz, M., Greenberg, C. R., and Elpeleg, O. N. (1998) Glutaryl-CoA dehydrogenase mutations in glutaric acidemia (type I): Review and report of thirty novel mutations. *Hum. Mutat. 12*, 141–144.
4. Westover, J. B., Goodman, S. I., and Frerman, F. E. (2003) Pathogenic mutations in the carboxyl-terminal domain of glutaryl-CoA dehydrogenase: Effects on catalytic activity and the stability of the tetramer. *Mol. Genet. Metab. 79*, 245–256.
5. Boll, M., Fuchs, G., and Heider, J. (2002) Anaerobic oxidation of aromatic compounds and hydrocarbons. *Curr. Opin. Chem. Biol. 6*, 604–611.
6. Carmona, M., Zamarro, M. T., Blazquez, B., Durante-Rodriguez, G., Juarez, J. F., Valderrama, J. A., Barragan, M. J., Garcia, J. L., and Diaz, E. (2009) Anaerobic catabolism of aromatic compounds: A genetic and genomic view. *Microbiol. Mol. Biol. Rev. 73*, 71–133.
7. Fuchs, G. (2008) Anaerobic metabolism of aromatic compounds. *Ann. N.Y. Acad. Sci. 1125*, 82–99.
8. Blazquez, B., Carmona, M., Garcia, J. L., and Diaz, E. (2008) Identification and analysis of a glutaryl-CoA dehydrogenase-encoding gene and its cognate transcriptional regulator from Azoarcus sp. CIB. *Environ. Microbiol. 10*, 474–482.
9. Härtel, U., Eckel, E., Koch, J., Fuchs, G., Linder, D., and Buckel, W. (1993) Purification of glutaryl-CoA dehydrogenase from *Pseudomonas* sp., an enzyme involved in the anaerobic degradation of benzoate. *Arch. Microbiol. 159*, 174–181.
10. Wischgoll, S., Heintz, D., Peters, F., Erxleben, A., Sarnighausen, E., Reski, R., Van Dorsselaer, A., and Boll, M. (2005) Gene clusters involved in anaerobic benzoate degradation of *Geobacter metallireducens*. *Mol. Microbiol. 58*, 1238–1252.
11. Wischgoll, S., Taubert, M., Peters, F., Jehmlich, N., von Bergen, M., and Boll, M. (2009) Decarboxylating and nondecarboxylating glutaryl-coenzyme A dehydrogenases in the aromatic metabolism of obligately anaerobic bacteria. *J. Bacteriol. 191*, 4401–4409.
12. Dwyer, T. M., Rao, K. S., Goodman, S. I., and Frerman, F. E. (2000) Proton abstraction reaction, steady-state kinetics, and oxidation-reduction potential of human glutaryl-CoA dehydrogenase. *Biochemistry 39*, 11488–11499.
13. Dwyer, T. M., Rao, K. S., Westover, J. B., Kim, J. J., and Frerman, F. E. (2001) The function of Arg-94 in the oxidation and decarboxylation of glutaryl-CoA by human glutaryl-CoA dehydrogenase. *J. Biol. Chem. 276*, 133–138.

14. Fu, Z., Wang, M., Paschke, R., Rao, K. S., Frerman, F. E., and Kim, J. J. (2004) Crystal structures of human glutaryl-CoA dehydrogenase with and without an alternate substrate: Structural bases of dehydrogenation and decarboxylation reactions. *Biochemistry 43*, 9674–9684.
15. Gomes, B., Fendrich, G., and Abeles, R. H. (1981) Mechanism of action of glutaryl-CoA and butyryl-CoA dehydrogenases. Purification of glutaryl-CoA dehydrogenase. *Biochemistry 20*, 1481–1490.
16. Rao, K. S., Albro, M., Dwyer, T. M., and Frerman, F. E. (2006) Kinetic mechanism of glutaryl-CoA dehydrogenase. *Biochemistry 45*, 15853–15861.
17. Rao, K. S., Fu, Z., Albro, M., Narayanan, B., Baddam, S., Lee, H. J., Kim, J. J., and Frerman, F. E. (2007) The effect of a Glu370Asp mutation in glutaryl-CoA dehydrogenase on proton transfer to the dienolate intermediate. *Biochemistry 46*, 14468–14477.
18. Rao, K. S., Albro, M., Zirrolli, J. A., Vander Velde, D., Jones, D. N., and Frerman, F. E. (2005) Protonation of crotonyl-CoA dienolate by human glutaryl-CoA dehydrogenase occurs by solvent-derived protons. *Biochemistry 44*, 13932–13940.
19. Peters, F., Rother, M., and Boll, M. (2004) Selenocysteine-containing proteins in anaerobic benzoate metabolism of *Desulfococcus multivorans*. *J. Bacteriol. 186*, 2156–2163.
20. Beatrix, B., Bendrat, K., Rospert, S., and Buckel, W. (1990) The biotin-dependent sodium ion pump glutaconyl-CoA decarboxylase from *Fusobacterium nucleatum* (subsp. *nucleatum*). Comparison with the glutaconyl-CoA decarboxylases from Gram-positive bacteria. *Arch. Microbiol. 154*, 362–369.
21. Boiangiu, C. D., Jayamani, E., Brugel, D., Herrmann, G., Kim, J., Forzi, L., Hedderich, R., Vgenopoulou, I., Pierik, A. J., Steuber, J., and Buckel, W. (2005) Sodium ion pumps and hydrogen production in glutamate fermenting anaerobic bacteria. *J. Mol. Microbiol. Biotechnol. 10*, 105–119.
22. Buckel, W. (2001) Sodium ion-translocating decarboxylases. *Biochim. Biophys. Acta 1505*, 15–27.
23. Otwinowski, Z., and Minor, W. (1997) Processing of X-ray diffraction data collected in oscillation mode. *Methods Enzymol. 276*, 307–326.
24. Kabsch, W. (1993) Automatic processing of rotation diffraction data from crystals of initially unknown symmetry and cell constants. *J. Appl. Crystallogr. 26*, 795–800.
25. McCoy, A. J., Grosse-Kunstleve, R. W., Adams, P. D., Winn, M. D., Storoni, L. C., and Read, R. J. (2007) Phaser crystallographic software. *J. Appl. Crystallogr. 40*, 658–674.
26. Murshudov, G. N., Vagin, A. A., and Dodson, E. J. (1997) Refinement of macromolecular structures by the maximum-likelihood method. *Acta Crystallogr. D53*, 240–255.
27. Emsley, P., and Cowtan, K. (2004) Coot: Model-building tools for molecular graphics. *Acta Crystallogr. D60*, 2126–2132.
28. Laskowski, R. A., Moss, D. S., and Thornton, J. M. (1993) Main-chain bond lengths and bond angles in protein structures. *J. Mol. Biol. 231*, 1049–1067.
29. Makarova, O., Kamberov, E., and Margolis, B. (2000) Generation of deletion and point mutations with one primer in a single cloning step. *BioTechniques 29*, 970–972.
30. Johnson, M., Zaretskaya, I., Raytselis, Y., Merezhuk, Y., McGinnis, S., and Madden, T. L. (2008) NCBI BLAST: A better web interface. *Nucleic Acids Res. 36*, W5–W9.
31. Larkin, M. A., Blackshields, G., Brown, N. P., Chenna, R., McGettigan, P. A., McWilliam, H., Valentin, F., Wallace, I. M., Wilm, A., Lopez, R., Thompson, J. D., Gibson, T. J., and Higgins, D. G. (2007) Clustal W and Clustal X version 2.0. *Bioinformatics 23*, 2947–2948.
32. Waterhouse, A. M., Procter, J. B., Martin, D. M., Clamp, M., and Barton, G. J. (2009) Jalview Version 2: A multiple sequence alignment editor and analysis workbench. *Bioinformatics 25*, 1189–1191.
33. Battaile, K. P., Nguyen, T. V., Vockley, J., and Kim, J. J. (2004) Structures of isobutyryl-CoA dehydrogenase and enzyme-product complex: Comparison with isovaleryl- and short-chain acyl-CoA dehydrogenases. *J. Biol. Chem. 279*, 16526–16534.
34. Ghisla, S., and Thorpe, C. (2004) Acyl-CoA dehydrogenases. A mechanistic overview. *Eur. J. Biochem. 271*, 494–508.
35. Rao, K. S., Albro, M., Vockley, J., and Frerman, F. E. (2003) Mechanism-based inactivation of human glutaryl-CoA dehydrogenase by 2-pentynoyl-CoA: Rationale for enhanced reactivity. *J. Biol. Chem. 278*, 26342–26350.